ORAL & IMPLANTOLOGY

original research article

Correlation between coronal and apical arch form and degree of divergence: a volumetric computed tomography analysis

L. LOMBARDO[1], F. VERONESI[1], V. CANDOTTO[2], M. NARDONE[3], G. SICILIANI[1]

[1] *Department of Orthodontics, University of Ferrara, Ferrara, Italy*
[2] *Department of Biomedical, Surgical and Dental Sciences, University of Milan, Milan, Italy*
[3] *Ministry of Public Health, Rome, Italy*

SUMMARY
Purpose. To determine the existence of any correlation between the degree of divergence and apical and coronal arch form using cone-beam computed tomography (CBCT).
Materials and methods. A total of 176 (88 coronal and 88 apical) CBCT scans pertaining to a sample of 44 subjects (16 males and 28 females), of which 26 were Class I, 14 Class II and 4 Class III, were analysed. A lateral projection of the skull was obtained from each VCT and cephalometric tracing was performed (according to Ricketts) so as to divide the sample into subgroups based on the degree of divergence (11 short-faced, 18 norm-faced and 15 long-faced subjects). Dahlberg's index values were calculated and Student's t-test for paired data was applied.
Results. On the whole, the hyperbolic cosine curve was found to be the most representative of the arch forms considered.
Conclusions. A correlation between degree of divergence and the arch form of the apical and, especially, coronal portions of both the upper and lower jaws was revealed.

Key words: arch form, divergence, CBCT.

Introduction

Geometric constructions (1, 2) and qualitative evaluation (3-5) have been used for over a century to study the dental arch form, which has been described in terms of ellipses (6-9), catenary curves (10), polynomial functions (11, 12), parabolas (13), and cubic splines (14). Mathematical methods used to test the goodness-of-fit of these curves to the dental arcade include minimum chi-squared fitting and the innovative average fitting technique, in which the fit of the arch forms is calculated on the average arch.
In 1934, Chuck (5) classified the arch forms into tapered, square and ovoid, and a review of relevant literature (5, 15, 16) permits us to conclude that, in Caucasian subjects, the prevalence of these shapes is as follows: 45% tapered, 10% square and 45% ovoid.
Despite this deceptively simple classification, however, the search for an ideal arch form, or forms, that can be applied to every single patient, or group of patients, has proved unrealistic due to the vast range of individual variation within the population (17). The shape of the arches is determined by not only the underlying bone, but also the oral musculature and the functional forces at play. Indeed, according to equilibrium theory (17), the light, prolonged pres-

sure exerted by the lip, teeth and tongue greatly affect the position of the teeth. The degree of muscle activity, on the other hand, has little or no influence on the dental morphology, but does affect the density of the supporting bone. In particular, hyperdivergent subjects have been shown to present a hypotonic muscular component, whereas hypodivergent subjects tend to feature hypertonic musculature.

It is unsurprising therefore, that various studies (18, 19) have been conducted in the attempt to find a correlation between arch form and facial type. These have reported narrower arch forms in long-faced with respect to short-faced subjects. Furthermore, it has also been noted that Class I and II subjects present narrower arch forms than those in Class III.

The advent of precise three-dimensional imaging techniques has revolutionized studies such as these, which used to rely on the comparatively imprecise measurement of plaster models. Furthermore, volumetric tomography has made it possible not only to measure the visible portions of the teeth, but also those previously hidden from view, i.e. the roots. In a VCT (volumetric computed tomography) study conducted in 2007 (20), the positions of both the coronal and apical sections of the teeth were determined and used to estimate their respective arch forms, revealing that the shape of the apical arches is roughly elliptical while the coronal arches can only be represented by means of a shape featuring a change in curvature.

With a view to expanding on these results, the aim of the present study was to identify any relationship between arch form and degree of divergence. This was performed by evaluating the position of the crowns and root apices with the aid of VCT. Indeed, as previously mentioned, this technique allows us to study the position of the root apices, which were not previously easily measurable and have therefore not been studied extensively, despite their being a fundamental component in the planning of effective and stable orthodontic treatment. Furthermore, dental cone-beam computed tomography (CBCT) has the added advantage of exposing the patient to considerably (roughly 5 times) less radioactivity with respect to conventional CT (21-24).

Materials and methods

An initial database of almost 1800 VCTs was consulted, and a sample of 44 VCTs, belonging to 16 males and 28 females, was selected as appropriate for this study. The sample included patients with the following characteristics: no previous orthodontic treatment; no extensive restoration; one or both arches in the permanent dentition; presence of the first permanent molars and no visible intraoral or extraoral asymmetry.

This sample was composed of 26 (59%) Class I, 14 (32%) Class II and 4 (9%) Class III subjects. The degree of crowding was, on average, 1.37 (Little's index) and ranged from 0.4 and 2.85 (little crowding). All patients were Caucasian and the mean age was 21.6 years.

Tomographic images of the upper and lower jaws of each of the 44 patients, a total of 88 arches, were analysed. Apical and coronal scans of each arch were considered, and the total sample therefore comprised 176 VCT images. All VCTs were taken using the same cone-beam DVT appliance, NewTom 3G, manufactured by the firm QR, Verona.

A lateral projection of the skull was obtained from each VCT and subjected to cephalometric tracing, used to subdivide the sample according to degree of divergence. The cephalometric analysis technique chosen for this study was that proposed by Ricketts, considering the facial axis angle, i.e. the angle formed between the cranial base Ba-Na and the facial axis Pt-Gn. This angle shows the growth trajectory of the mandible. After cephalometric tracing on laterolateral projections of the selected VCTs, the sample was divided into three divergence groups, composed as follows: 11 short-faced subjects (facial axis angle ≥93°), 18 norm-faced subjects (facial axis angle 90°±3) and 15 long-faced subjects (facial axis angle ≤87°).

Axial renderings of the VCTs pertaining to these

patients were then acquired via NNT software appropriate for the volumetric tomograph employed. The axial planes were oriented according to Downs, who defined the occlusal plane as that containing the lines passing through the central occlusal point of the first molars and incisors. Accordingly, two sections per arch were considered: a coronal section, passing through the point of contact between the lateroposterior teeth (Figures 1, 2, for the upper arch and figures 5, 6 for the lower arch), and an apical section taken 10 mm from the coronal section in all cases (Figures 3, 4, for the upper arch and figures 7, 8 for the lower arch) in order to guarantee homogeneity of the subsequent measurements; this value was selected as the border of the apical third, on the basis of the mean of the root lengths of all permanent teeth, considering that the coronal sections were taken at roughly the dental equator.
These slices were then used to construct, for each patient, a PowerPoint presentation comprising 4 slides, one of the coronal section of the upper arch, one of the coronal section of the lower arch, one of the apical section of the upper arch, and

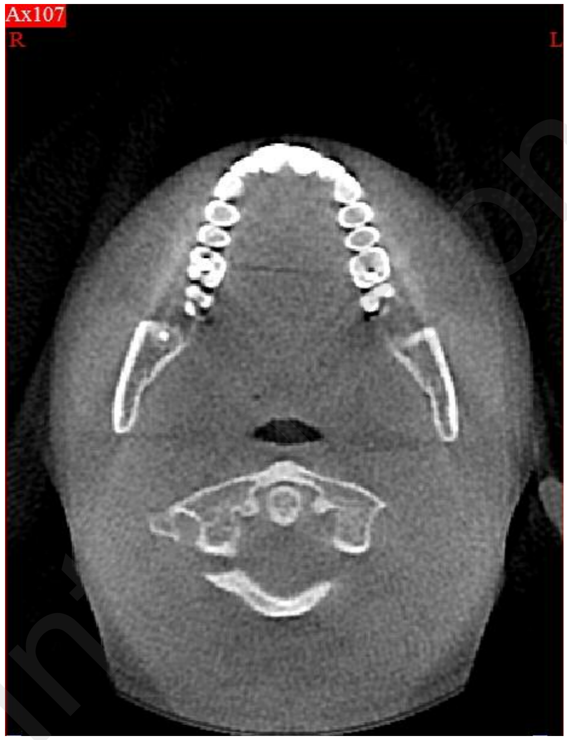

Figure 2
Axial slice of upper coronal arch form.


Figure 1
Axial section of upper coronal arch form, sagittal view.


Figure 3
Axial section of upper apical arch form, sagittal view.

Figure 4
Axial slice of upper apical arch form.

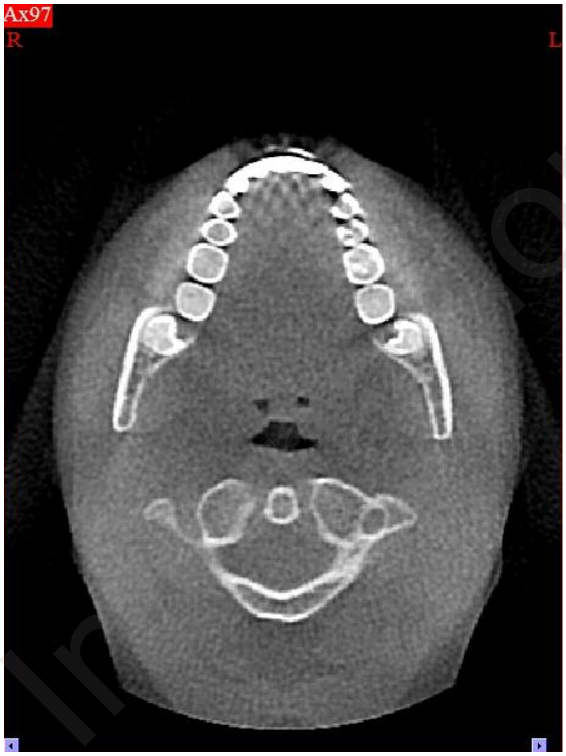

Figure 6
Axial slice of lower coronal arch form.

Figure 5
Axial section of lower coronal arch form, sagittal view.

Figure 7
Axial section of lower apical arch form, sagittal view.

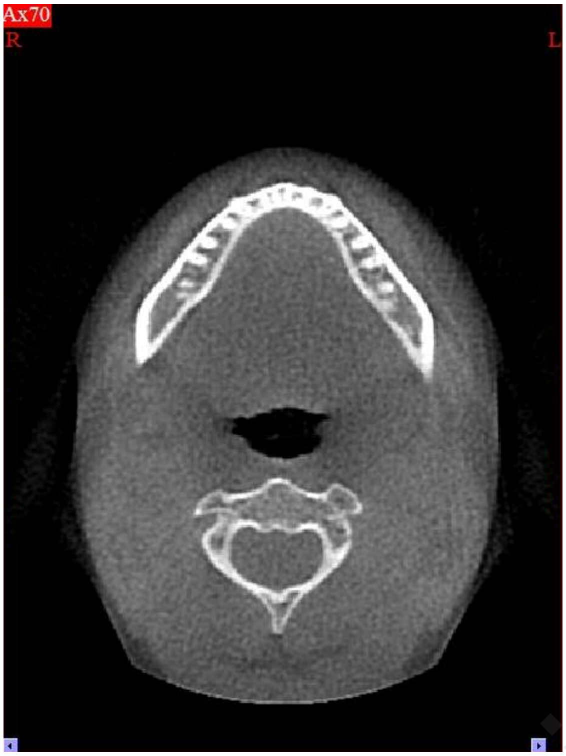

Figure 8
Axial slice of lower apical arch form.

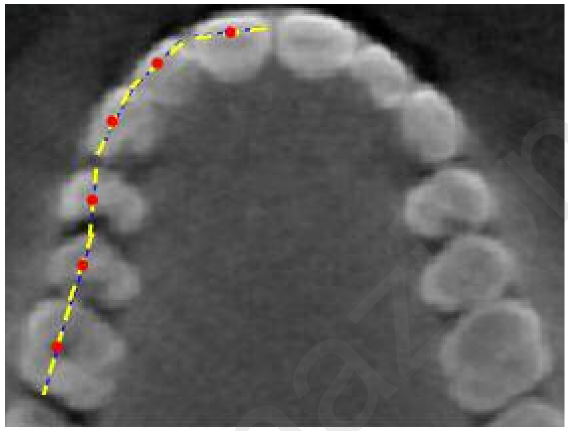

Figure 9
Coronal position markers.

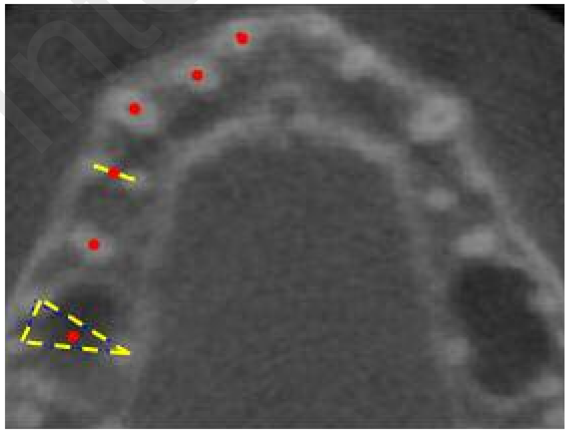

Figure 10
Apical position markers.

one of the apical section of the lower arch.
Each dental crown and root apex on these images was then marked at selected reference points; as Andrews (25) (1972) and White (26) (1978) both agreed that the curve best representing the arch form is that obtained by joining the points of interproximal contact, the coronal markers were positioned at the central points of the maximal mesiodistal diameter of the crowns, i.e. at points equidistant from the interproximal contact points (Figure 9). The apical points, on the other hand, were positioned at the centre of the root tip in monoradicular teeth, at the point equidistant from the two root tips in biradicular teeth, and the barycentre of the triangle formed by the three root tips in triradicular teeth (Figure 10).
So as to obtain symmetrical arches with respect to the vertical axis, in addition to including only patients with symmetrical arches in the initial selection, it was necessary in several cases to rotate the image so that the first molar markers (coronal and apical) were horizontally aligned (Figure 11). Linear rescaling was used to transform the coordinates so as to equalize the horizontal distance between the two first molars in all arches, so that individual variation in jaw size could be excluded from the later comparison (Figures 12, 13).
The coordinates of the reference points were then entered on appositely created Excel spreadsheets which were used as the basis for subsequent calculations and graphical representations with the aim of defining the best fit of the average dental arch among the three curves consid-

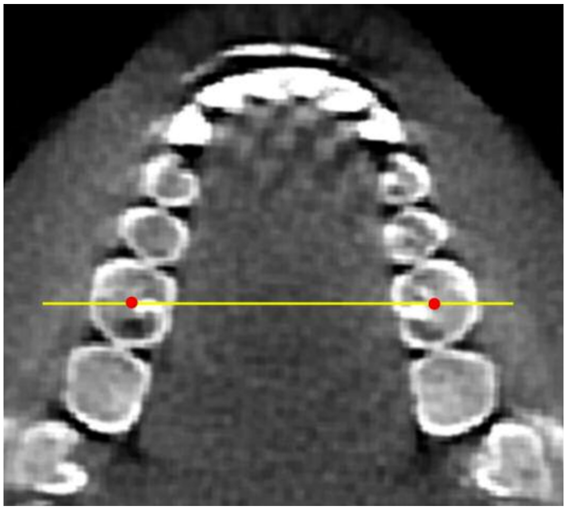

Figure 11
Horizontal alignment of first molars.

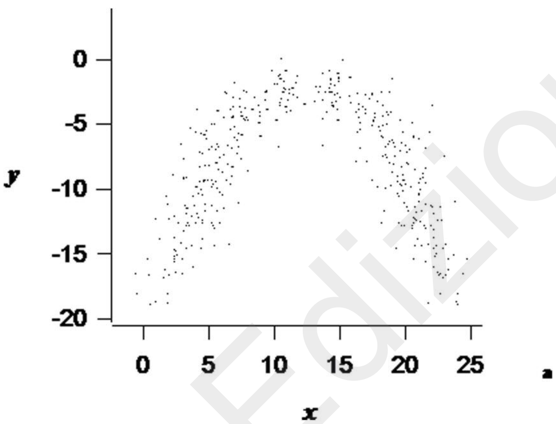

Figure 12
Example arch before rescaling.

ered (hyperbolic cosine, ellipse, parabola).
The next stage in the procedure was to create a scatter plot of the points representative of each tooth for each arch considered. The mean position and standard deviation of each tooth were calculated and used to identify a continuous curve representing the average arch form passing through the mean position of each group of coordinates. A mathematical tool known as min-

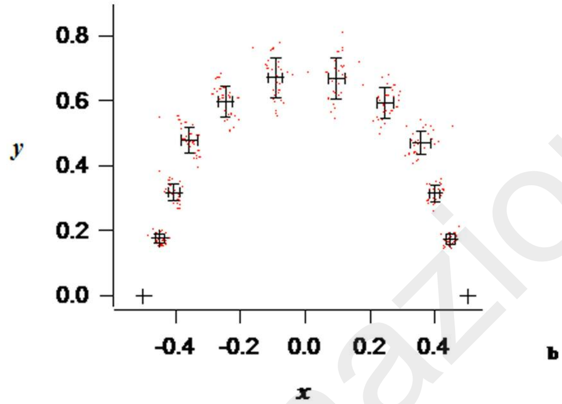

Figure 13
Arch after rescaling.

imum χ^2 (chi-square) was used to this end. For each arch the fits were generated for the following curves: parabola, ellipse and hyperbolic cosine (Table 1) and χ^2 was calculated to determine their goodness-of-fit.

Statistical analysis

All measurements were repeated by the same operator, using the same computer, software and working conditions, after approximately 1 month from the initial measurement session, and Dahlberg's d test was used for measurement systems analysis. The statistically significance of this test was then analysed by means of Student's t-test for paired data (Table 2), which revealed no statistically significant discrepancy linked to the measurement procedure, i.e. initial calculation of the mean position of each tooth and then determination of the mean coronal and apical arch forms. The reliability of measurement of each of the markers considered was thereby confirmed.
This analysis was performed separately for each arch (upper coronal, lower apical, etc.) in each group of patients, thereby furnishing a single fit for each average arch found. In other words, an

Table 1 - Curves fitted: their Cartesian equations and corresponding fit parameters.

CURVE	EQUATION	FIT PARAMETERS
Symmetric parabola for $(x,y)=(\pm 1/2, 0)$	$y_{fit}=p_1\left[1-4x^2\right]$	p_1
Ellipse for $(x,y)=(\pm 1/2, 0)$	$y_{fit}=p_1\left\{\sqrt{\left[1-\left(\frac{x}{p_2}\right)^2\right]}-\sqrt{\left[1-\left(\frac{1}{2p_2}\right)^2\right]}\right\}$	p_1, p_2
Hyperbolic cosine for $(x,y)=(\pm 1/2, 0)$	$y_{fit}=p_1\left[\cosh\left(\frac{1}{2p_2}\right)-\cosh\left(\frac{x}{p_2}\right)\right]$	p_1, p_2

Table 2 - Example of Dahlberg's index and Student's t-test calculated for one subject.

Variable	Statistical Description	
	Dahlberg's Index	*Statistical Significance*
Upper apices x	0.000833	Not significant
Upper apices y	0.000833	Not significant
Upper crowns x	0.004583	Not significant
Upper crowns y	0.001250	Not significant
Lower crowns x	0.000417	Not significant
Lower crowns y	0.001250	Not significant
Lower apices x	0.000833	Not significant
Lower apices y	0.001667	Not significant

average fit was performed, thereby reducing the method error.

Results

In the group comprising the short-faced subjects (Figure 14), no statistically significant difference between apical and coronal arch forms was revealed. Although the parabola fit was slightly more appropriate to the apical mandibular arch than the other arches considered, on the whole, it did not prove a good representation of the coronal or apical arch forms in either the upper or lower jaw. In contrast, both the ellipse and hyperbolic cosine showed excellent fit for the upper and lower apical and coronal arch forms. Nonetheless, it should be noted that neither of these curves perfectly represented the shape of the canine areas, whose curvature is different to the posterior sectors. Thus, due to its significant change in curvature, the hyperbolic cosine fit was the better of the two on the whole, even though for the apical mandibular arch, comparison of the values for χ^2 (Table 3) showed that the two curves were very similar in practical terms: 1.532223 (hyperbolic cosine) with respect to 1.616714 (ellipse).

In normodivergent subjects (Figure 15), a moderately significant difference between apical and coronal arch forms was revealed. The curve

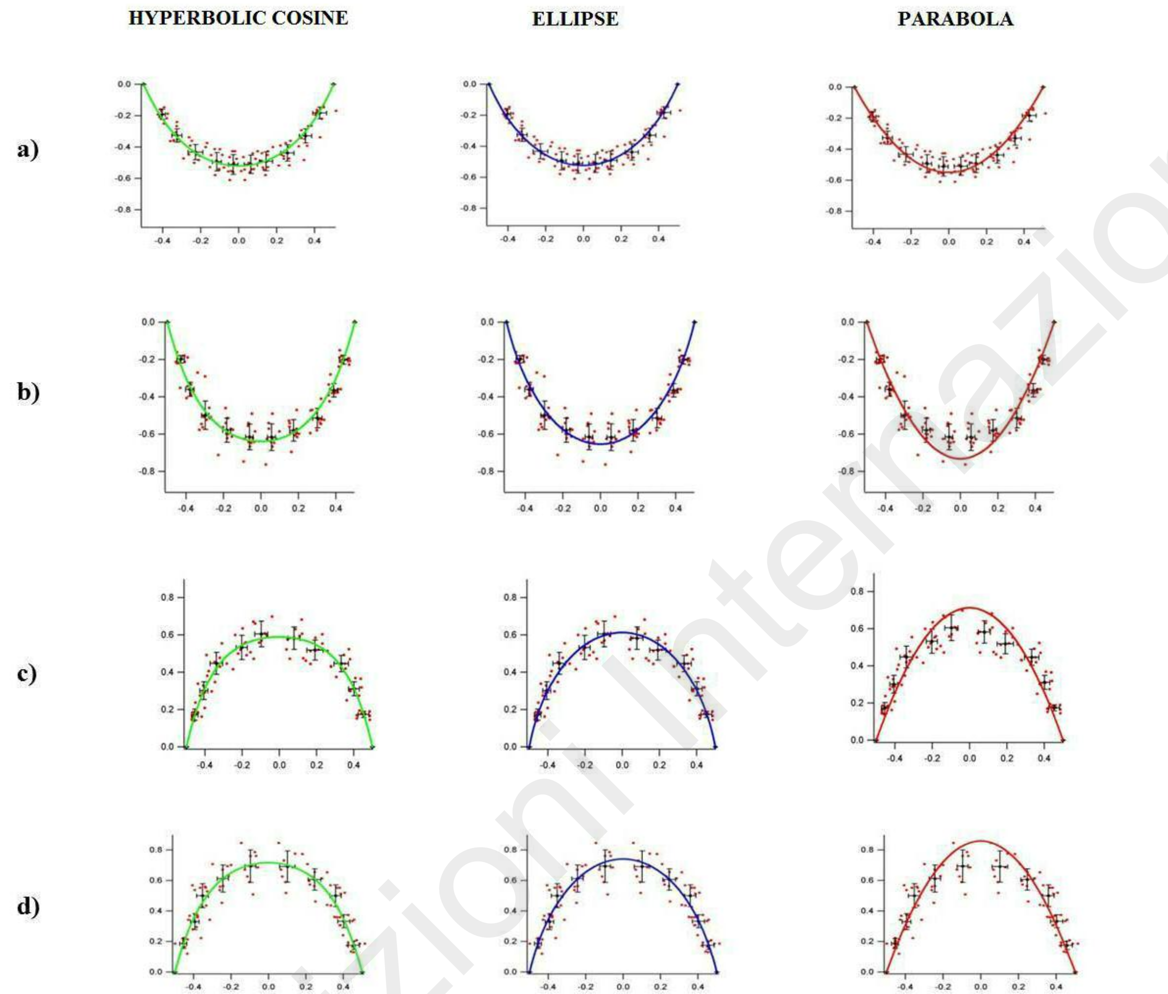

Figure 14
Short-faced subject group results. a) Mean apical mandibular arch fit: hyperbolic cosine, ellipse, parabola; b) Mean coronal mandibular arch fit: hyperbolic cosine, ellipse, parabola; c) Mean apical maxillary arch fit: hyperbolic cosine, ellipse, parabola; d) Mean coronal maxillary arch fit: hyperbolic cosine, ellipse, parabola.

that best fit the apical and coronal portions of the lower arch was the hyperbolic cosine, while that which was least representative of the position of the teeth was the parabola. The ellipse provided a fairly adequate representation of the apical lower arch, but the hyperbolic cosine was superior in this respect, even though this also failed to provide a perfect fit to the apical and coronal arches as, in both cases, χ^2 was found to be greater than 4.

As regards the upper arch, the best fit was found to be the hyperbolic cosine, in both apical and coronal portions, while once again the parabola was the least representative curve. In particular (Table 4), a marked difference was evident between the χ^2 of the hyperbolic cosine in the apical portion of the upper arch, 0.7781621 (very good fit) and the corresponding χ^2 of the parabola 14.75837 (very poor fit). At the mandibular root apices, the hyperbolic cosine was a very good fit, whereas in the coronal curve, a considerable discrepancy between the position of the canines and this curve was evidenced. The elliptical curve, on the other hand, was also found to be representative of the apical and coronal portions of the upper and lower arches, although the

Table 3 - Hyperbolic cosine, ellipse and parabola goodness-of-fit (c^2), fit parameters (p_1 and p_2) and corresponding errors (Dp_1 and Dp_2) for mean coronal and apical maxillary and mandibular arches in short-faced subjects.

	Hyperbolic cosine				Ellipse				Parabola			
	Upper crowns	**Upper apices**	**Lower crowns**	**Lower apices**	**Upper crowns**	**Upper apices**	**Lower crowns**	**Lower apices**	**Upper crowns**	**Upper apices**	**Lower crowns**	**Lower apices**
X^2	1.488298	0.8549607	4.606206	1.532223	1.801772	1.885303	5.581513	1.616714	9.591539	24.33792	16.53252	3.438401
p_1	0.0892276	0.03804493	-0.1097006	-0.204308	1.242279	0.8721598	-1.205948	-1.285658	0.8584214	0.7124274	-0.7319354	-0.5493138
Δp_1	0.07833923	0.02416739	0.0703204	0.2350775	0.368794	0.1475282	0.3243521	0.8344186	0.03982409	0.0265527	0.02542373	0.02249322
p_2	0.1729596	0.14308	0.191706	0.2578834	0.546541	0.5236976	0.5624617	0.6208386				
Δp_2	0.043119	0.02265421	0.03771434	0.1103072	0.03756194	0.01554684	0.04035606	0.1412051				

Table 4 - Hyperbolic cosine, ellipse and parabola goodness-of-fit (c^2), fit parameters (p. and p^1 and p_2) and corresponding errors (Dp_1 and Dp_2) for mean coronal and apical maxillary and mandibular arches in norm-faced subjects.

	Hyperbolic cosine				Ellipse				Parabola			
	Upper crowns	**Upper apices**	**Lower crowns**	**Lower apices**	**Upper crowns**	**Upper apices**	**Lower crowns**	**Lower apices**	**Upper crowns**	**Upper apices**	**Lower crowns**	**Lower apices**
X^2	3.282019	0.7781621	7.543277	4.158337	3.721106	1.497714	9.015923	4.925707	7.57687	14.75837	19.56189	14.36304
p_1	0.3182929	0.06777585	-0.1440976	-0.167676	2.242927	1.005069	-1.357292	-1.187463	0.8780462	0.7179523	-0.709293	-0.54945
Δp_1	0.2644989	0.04605262	0.0833372	0.09047507	1.094389	0.2269065	0.3826554	0.3537266	0.02905751	0.02537763	0.01974845	0.01176256
p_2	0.2618136	0.1666179	0.2107466	0.2410259	0.6545063	0.5380384	0.5860728	0.6064984				
Δp_2	0.07809388	0.03176781	0.03990888	0.04637742	0.1111563	0.02713843	0.05028496	0.06023085				

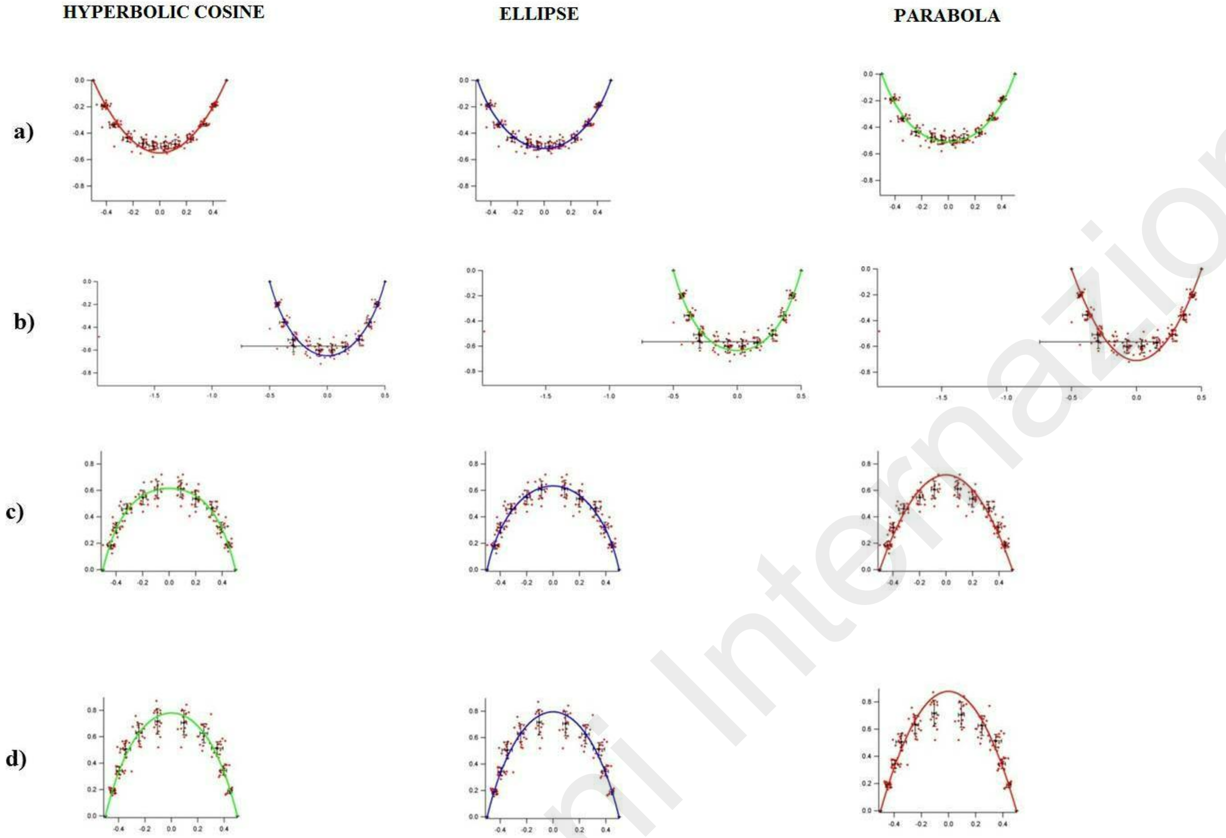

Figure 15
Norm-faced subject group results. a) Mean apical mandibular arch fit: hyperbolic cosine, ellipse, parabola; b) Mean coronal mandibular arch fit: hyperbolic cosine, ellipse, parabola; c) Mean apical maxillary arch fit: hyperbolic cosine, ellipse, parabola; d) Mean coronal maxillary arch fit: hyperbolic cosine, ellipse, parabola.

hyperbolic cosine, featuring a marked change in curvature, was found to be superior in this respect.

In long-faced subjects (Figure 16), no statistically significant difference was detected between the coronal and apical curves. In the upper arch, the hyperbolic cosine was the best-fitting curve in both coronal and apical portions. The ellipse was a fairly adequate representation of the coronal arch, but displayed a poor fit at the mandibular apices (a particularly large discrepancy between mean apical and coronal positions in the premolar regions), with a χ^2 of 15.67413 with respect to the 1.011527 of the hyperbolic cosine (Table 5).

The best fit at the mandibular apices was seen with the hyperbolic cosine, whereas the parabola was a poor fit in both the crowns and root apices of the lower arch. The hyperbolic cosine was the best-fitting curve at the maxillary crowns, whereas the ellipse was more representative of the apical arch form. Nevertheless, it should be noted that no great difference was seen between the two types of fit in the upper apical arch in terms of χ^2, which was adequate for both the ellipse (1.530169) and the hyperbolic cosine (1.842981). At the upper coronal arch, on the other hand, the position of the ellipse differed from the mean position of the teeth, especially in the anterior portion of the arch (from canine to canine). In contrast, the hyperbolic cosine was extremely representative of the entire coronal arch, it being characterized by a change in curvature corresponding to the anterior sector.

original research article

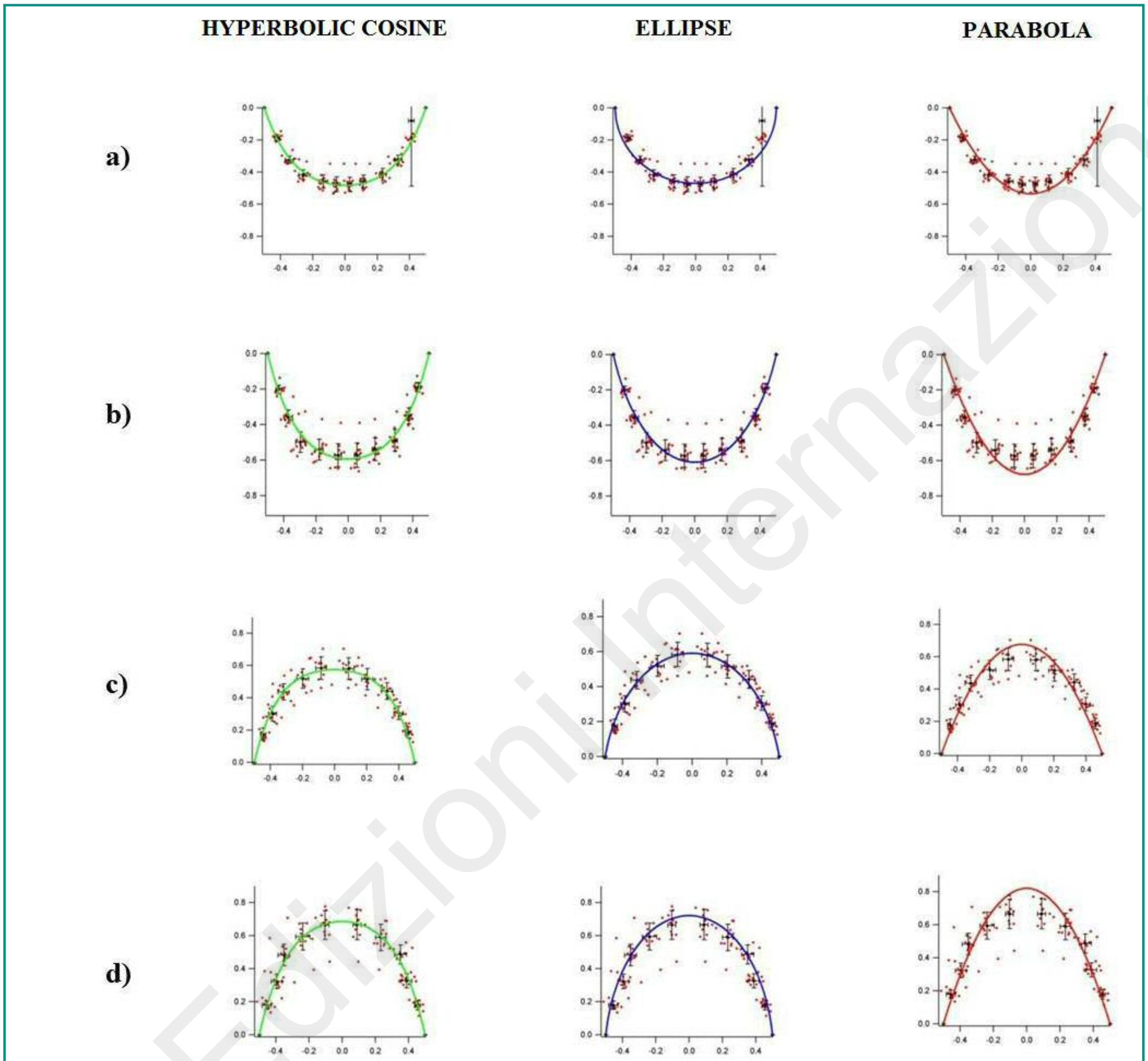

Figure 16
Long-faced subject group results. a) Mean apical mandibular arch fit: hyperbolic cosine, ellipse, parabola; b) Mean coronal mandibular arch fit: hyperbolic cosine, ellipse, parabola; c) Mean apical maxillary arch fit: hyperbolic cosine, ellipse, parabola; d) Mean coronal maxillary arch fit: hyperbolic cosine, ellipse, parabola.

Discussion

Various Authors have documented associations between long-faced subjects and a long, narrow arch form, short-faced subjects and relatively wide arches, and normodivergent subjects with a paraboloid arch form (18, 19). However, these considerations were all made based on measurements of arch form and dental position performed on plaster models, and therefore only the coronal section of the arches.
In contrast, this study, thanks to VCT technology, was able to make accurate measurement not only of the coronal portion of the arches, but also of the root apices. Furthermore, by means of a rescaling procedure it was possible to ensure that all measurements were made on arches of the

Table 5 - Hyperbolic cosine, ellipse and parabola goodness-of-fit (c^2), fit parameters (p_1 and p_2) and corresponding errors (Dp_1 and Dp_2) for mean coronal and apical maxillary and mandibular arches in long-faced subjects.

	Hyperbolic cosine				Ellipse				Parabola			
	Upper crowns	Upper apices	Lower crowns	Lower apices	Upper crowns	Upper apices	Lower crowns	Lower apices	Upper crowns	Upper apices	Lower crowns	Lower apices
X^2	2.21907	1.842981	2.134684	1.011527	16.0824	1.530169	3.119666	15.67413	11.54555	13.76602	12.85567	12.61916
p_1	0.0864924	0.03965309	-0.0869674	-0.0707371	0.875932	0.7887639	-1.065472	-0.473866	0.8201304	0.6766212	-0.6777427	-0.5351791
Δp_1	0.0706032	0.03369344	0.06119654	0.0468502	0.131039	0.1672878	0.2987717	0.0613576	0.0353077	0.0286268	0.0254779	0.0154313
p_2	0.1736873	0.1456856	0.182002	0.1820854	0.508033	0.516556	0.5532771	0.5000131				
Δp_2	0.0403733	0.03168488	0.03825461	0.0366211	0.007677	0.0176026	0.0397514	0.0003586				

same virtual size, thereby providing a homogeneous sample as regards arch size. Using this methodology, the coronal arches, and to a lesser extent the apical arches, were shown to feature a change in curvature at the canines in all sample groups (short-faced, norm-faced and long-faced subjects). A further advantage of this type of study was that rather than relying on calculation of an average of fits, in this case we were able to determine the average fit, thereby reducing the method error.

In order to represent the coronal arch form, the most suitable fit was found to be, in all three degrees of divergence considered, the hyperbolic cosine, i.e. a curve of altering curvature. Likewise, the hyperbolic cosine was also found to be the most suitable means of representing the apical arch form in all three patient groups, although it must be mentioned that the ellipse also provided suitable fit, particularly in the lower apical arch in long-faced subjects. The worst fit, in both the upper and lower apical and coronal arches, was found to be the parabola in all sample groups (short- norm- and long-faced subjects).

Despite this general homogeneity, comparison of the best fits yielded for the three divergence groups did reveal several differences.

In particular, it was shown that the hyperbolic cosine was the most representative fit of the upper coronal arch form in long-faced subjects, even though this particular arch form was observed to be, on average, more "tapered" in the anterior sector (from canine to canine) with respect to the corresponding apical arch form, which is best represented by an ellipse. This can be explained by the hypotonic musculature characteristic of hyperdivergent subjects that wields more influence on the dental crowns with respect to the roots (27). The hyperbolic cosine was without doubt the curve that best fit the mandibular coronal arch as compared to that of the maxilla. In fact, in the hyperdivergent subjects, who are prone to open-bite and nasal respiration, the tongue tends to have a low position, the orbicular muscle of the mouth tends towards hypotonicity and little pressure is therefore exerted on the maxillary coronal arch,

which is generally more contracted than its mandibular counterpart (28).
In short-faced subjects, the hyperbolic cosine (a wide arch with a change in curvature at the canines) was also found to be the curve of best fit, in this case of all arch forms considered (upper, lower, coronal, apical), especially in the case of the maxillary coronal arch. In fact, hypodivergent patients tend to be characterized by a flattened oral vault and hypertonic orbicular muscles and tongue (this muscular component plays an important role in determining the development of the dentomaxillary complex and, in particular, "moulds" the upper jaw, favouring transversal growth) (29). Thus the upper coronal arch has a wider appearance.
In norm-faced subjects, the most representative arch form, in both coronal and apical portions of the maxilla and mandible, was also the hyperbolic cosine. With respect to their long- and short-faced counterparts, these subjects have intermediate muscular and skeletal characteristics and, likewise, the fit of their arch form was also intermediate in nature with respect to the other sample groups, reflecting the balanced pattern of development in these subjects. In fact, normodivergent subjects are characterized by balanced muscle function, in which the masticatory, orbicular and tongue muscles therefore perform their functions without excesses of tension or relaxation, a situation that is obviously reflected in the development of the arch form (29). In addition it should be outline that syndromic and cleft patients have specific arch forms which should be analysed one by one (30-39).
In addition, the patient-related susceptibility is a critical factor for disease onset. So, every factor favouring oral biofilm formation (poor oral hygiene), host defence capability (smoking habit, excessive alcohol consumption, genetic traits, history of periodontitis, use of bisphosphonates), might favour developing of peri-implantis and periodontal disease in syndromic cleft patients, which diagnosis and treatment require dentist's engagement (40-62).

Conclusions

This VCT study revealed that there is a correlation between the degree of divergence and the shape of the upper and lower arches at both apical and, especially, coronal reference points.
The hyperbolic cosine was the most representative curve considered, although several differences in the mean position of the teeth in the various biotypes were noted.

References

1. Bonwill WGA. Geometrical and mechanical laws of articulation. Tr Odontol Soc Penn. 1884-1885, 119-133.
2. Hawley CA. Determination of the normal arch and its application in orthodontia. Dent Cosmos. 1905;47:541-552.
3. Williams PN. Determining the shape of the normal arch. Dental Cosmos. 1917;59:695-708.
4. McCoy DJ. A consideration of normal arch form and some of the methods of determining it. Int J Orthod. 1919;5:697-723.
5. Chuck GC. Ideal arch form. Angle Orthod. 1934;4:312-327.
6. Currier JH. A computerized geometric analysis of human dental arch form. Am J Orthod. 1969;56:164-179.
7. Sampson PD. Fitting conic sections to "very scattered" data: an iterative refinement of the Bookstein algorithm (Department of Statistics, University of Chicago, 1980).
8. Mutinelli S, Manfredi M, Cozzani M. A mathematic-geometric model to calculate variation in mandibular arch form. Eur J Orthod. 2000;22:113-125.
9. Mutinelli S, Cozzani M, Manfredi M, et al. Dental arch analysis system. Prog Orthod. 2004;5:200-211.
10. Mac CM, Scher EA. The ideal form of the human dental arcade, with some prosthetic application. Dent Rec (London). 1949;69:285-302, illust.
11. Ferrario VF, Sforza C, Miani A Jr., et al. Mathematical definition of the shape of dental arches in human permanent healthy dentitions. Eur J Orthod. 1994;16:287-294.
12. Pepe SH. Polynomial and catenary curve fits to human dental arches. J Dent Res. 1975;54:1124-1132.
13. Jones ML, Richmond S. An assessment of the fit of a parabolic curve to pre- and post-treatment dental arches. Br J Orthod. 1989;16:85-93.
14. BeGole EA. Application of the cubic spline function in the description of dental arch form. J Dent Res.

1980;59:1549-1556.
15. McLaughlin RP, Bennett JC. Arch form considerations for stability and esthetics. Revista Espana Ortodontica. 1999;29:46-63.
16. Nojima K, McLaughlin RP, Isshiki Y, et al. A comparative study of Caucasian and Japanese mandibular clinical arch forms. Angle Orthod. 2001;71:195-200.
17. Ronay V, Miner RM, Will LA, et al. Mandibular arch form: the relationship between dental and basal anatomy. Am J Orthod Dentofacial Orthop. 2008; 134:430-438.
18. Ricketts RM. Orthodontic diagnosis and planning. Place: Saunders.
19. Kageyama T, Dominguez-Rodriguez GC, Vigorito JW, et al. A morphological study of the relationship between arch dimensions and craniofacial structures in adolescents with Class II Division 1 malocclusions and various facial types. Am J Orthod Dentofacial Orthop. 2006;129:368-375.
20. Mannarini C. University of Ferrara. 2007.
21. Mozzo P, Procacci C, Tacconi A, et al. A new volumetric CT machine for dental imaging based on the cone-beam technique: preliminary results. Eur Radiol. 1998;8:1558-1564.
22. Hanazawa T, Sano T, Seki K, et al. Radiologic measurements of the mandible: a comparison between CT-reformatted and conventional tomographic images. Clin Oral Implants Res. 2004;15:226-232.
23. Hilgers ML, Scarfe WC, Scheetz JP, et al. Accuracy of linear temporomandibular joint measurements with cone beam computed tomography and digital cephalometric radiography. Am J Orthod Dentofacial Orthop. 2005;128:803-811.
24. Winter AA, Pollack AS, Frommer HH, et al. Cone beam volumetric tomography vs. medical CT scanners. N Y State Dent J. 2005;71:28-33.
25. Andrews LF. The six keys to normal occlusion. Am J Orthod. 1972;62:296-309.
26. White LW. Individualized ideal arches. J Clin Orthod. 1978;12:779-787.
27. Kiliaridis S. Masticatory muscle influence on craniofacial growth. Acta Odontol Scand. 1995;53:196-202.
28. Proffit WR. Ortodonzia Moderna. Place: Ed. Masson 2001.
29. Giannì E. Rivisitazione ortognatodontica. Place: Piccin, 2007.
30. Cura F, Böhmer AC, Klamt J, et al. Replication analysis of 15 susceptibility loci for nonsyndromic cleft lip with or without cleft palate in an italian population. Birth Defects Research Part A - Clinical and Molecular Teratology. 2016;106:81-87.
31. Martinelli M, Girardi A, Cura F, et al. Non-syndromic cleft lip with or without cleft palate in Asian populations: Association analysis on three gene polymorphisms of the folate pathway. Archives of Oral Biology. 2016;61:79-82.
32. Nouri N, Memarzadeh M, Carinci F, et al. Family-based association analysis between nonsyndromic cleft lip with or without cleft palate and IRF6 polymorphism in an Iranian population. Clinical Oral Investigations. 2015;19:891-894.
33. Girardi A, Martinelli M, Cura F, et al. RFC1 and non-syndromic cleft lip with or without cleft palate: An association based study in Italy. Journal of Cranio-Maxillofacial Surgery. 2014;42:1503-1505.
34. Martinelli M, Girardi A, Cura F, et al. Evidence of the involvement of the DHFR gene in nonsyndromic cleft lip with or without cleft palate. European Journal of Medical Genetics. 2014;57:1-4.
35. Tettamanti L, Avantaggiato A, Nardone M, et al. Cleft palate only: Current concepts. ORAL & Implantology. 2017;10:45-52.
36. Tettamanti L, Avantaggiato A, Nardone M, et al. New insights in orofacial cleft: Epidemiological and genetic studies on Italian samples. ORAL & Implantology. 2017;10:11-19.
37. Caruso S, Storti E, Nota A, et al. Temporomandibular joint anatomy assessed by CBCT images. BioMed Research International. 2017;2017.
38. Giuca MR, Inglese R, Caruso S, et al. Craniofacial morphology in pediatric patients with Prader-Willi syndrome: a retrospective study. Orthodontics and Craniofacial Research. 2016;19:216-221.
39. Girardi A, Scapoli L, Cura F, et al. E-Cadherin coding gene (CDH1) and nonsyndromic cleft lip with or without cleft palate: Is there any association? Journal of Biological Regulators and Homeostatic Agents. 2015; 29:117-122.
40. Slutzkey S, Cohen O, Lauritano D, et al. Temperature changes of one-piece implants during the setting of acrylic resin temporary crown. The effect of implant diameter. An in vitro study. J Biol Regul Homeost Agents. 2017;31:53-60.
41. Matalon S, Frydman G, Lauritano D, et al. The effect of enriching denture adhesives with chlorhexidine diacetate on the proliferation of Candida albicans: an in vitro analysis. J Biol Regul Homeost Agents. 2017; 31:45-52.
42. Lopez MA, Andreasi Bassi M, Confalone L, et al. The use of resorbable cortical lamina and micronized collagenated bone in the regeneration of atrophic crestal ridges: a surgical technique. Case series. J Biol Regul Homeost Agents. 2016;30:81-85.
43. Conti P, Carinci F, Caraffa A, et al. Link between mast cells and bacteria: Antimicrobial defense, function and regulation by cytokines. Med Hypotheses. 2017; 106:10-14.
44. Ormianer Z, Solodukhin AL, Lauritano D, et al. Bilateral symmetry of anterior maxillary incisors: evaluation of a community-based population. J Biol Regul Homeost Agents. 2017;31:37-43.
45. Meirowitz A, Nowotny Klein R, Lauritano D, et al. Survey results of currently used techniques and materials by dentists for fabrication of complete removable den-

tal prostheses. J Biol Regul Homeost Agents. 2017; 31:27-36.
46. Lauritano D, Cura F, Candotto V, et al. Evaluation of the Efficacy of Titanium Dioxide with Monovalent Silver Ions Covalently Linked (Tiab) as an Adjunct to Scaling and Root Planing in the Management of Chronic Periodontitis Using Pcr Analysis: A Microbiological Study. J Biol Regul Homeost Agents. 2015; 29:127-130.
47. Lauritano D, Cura F, Gaudio RM, et al. Polymerase Chain Reaction to Evaluate the Efficacy of Silica Dioxide Colloidal Solutions in the Treatment of Chronic Periodontitis: A Case Control Study. J Biol Regul Homeost Agents. 2015, 29:131-135.
48. Lauritano D, Martinelli M, Mucchi D, et al. Bacterial load of periodontal pathogens among Italian patients with chronic periodontitis: A comparative study of three different areas. Journal of Biological Regulators and Homeostatic Agents. 2016;30:149-154.
49. Fanali S, Carinci F, Zolliiqo I, et al. One-piece implants installed in restored mandible: A retrospective study. European Journal of Inflammation. 2012;10:37-41.
50. Carinci F, Lauritano D, Cura F, et al. Prevention of bacterial leakage at implant-Abutment connection level: An in vitro study of the efficacy of three different implant systems. Journal of Biological Regulators and Homeostatic Agents. 2016;30:69-73.
51. Lauritano D, Petruzzi M, Nardi GM, et al. Single Application of a Dessicating Agent in the Treatment of Recurrent Aphthous Stomatitis. J Biol Regul Homeost Agents. 2015;29:59-66.
52. Scapoli L, Girardi A, Palmieri A, et al. Quantitative Analysis of Periodontal Pathogens in Periodontitis and Gingivitis. J Biol Regul Homeost Agents. 2015;29:101-110.
53. Lauritano D, Cura F, Candotto V, et al. Periodontal Pockets as a Reservoir of Helicobacter Pylori Causing Relapse of Gastric Ulcer: A Review of the Literature. J Biol Regul Homeost Agents. 2015;29:123-126.
54. Scapoli L, Girardi A, Palmieri A, et al. Interleukin-6 Gene Polymorphism Modulates the Risk of Periodontal Diseases. J Biol Regul Homeost Agents. 2015; 29: 111-116.
55. Lauritano D, Bignozzi CA, Pazzi D, et al. Evaluation of the efficacy of a new oral gel as an adjunct to home oral hygiene in the management of chronic periodontitis. A microbiological study using PCR analysis. Journal of Biological Regulators and Homeostatic Agents. 2016;30:123-128.
56. Roncati M, Lauritano D, Cura F, et al. Evaluation of light-emitting diode (led-835 nm) application over human gingival fibroblast: An in vitro study. Journal of Biological Regulators and Homeostatic Agents. 2016; 30:161-167.
57. Andreasi Bassi M, Lopez MA, Confalone L, et al. Clinical outcome of a two-piece implant system with an internal hexagonal connection: a prospective study. J Biol Regul Homeost Agents. 2016;30:7-12.
58. Baj A, Trapella G, Lauritano D, et al. An overview on bone recostruction of atrophic maxilla: Success parameters and critical issues. Journal of Biological Regulators and Homeostatic Agents. 2016;30:209-215.
59. Baj A, Muzio LL, Lauritano D, et al. Success of immediate versus standard loaded implants: A short literature review. Journal of Biological Regulators and Homeostatic Agents. 2016;30:183-188.
60. Lauritano D, Avantaggiato A, Candotto V, et al. Insulin activity on dental pulp stem cell differentiation: An in vitro study. Journal of Biological Regulators and Homeostatic Agents. 2015;29:48-53.
61. Avantaggiato A, Palmieri A, Carinci F, et al. Effects of glucosamine and nucleotide association on fibroblast: extracellular matrix gene expression. International journal of immunopathology and pharmacology. 2014; 27:689-693.
62. Baj A, Sollazzo V, Lauritano D, et al. Lights and shadows of bone augumentation in severe resorbed mandible in combination with implant dentistry. Journal of Biological Regulators and Homeostatic Agents. 2016;30:177-182.

Correspondence to:
Luca Lombardo, DDS
Department of Orthodontics
University of Ferrara
Via Montebello 31
44100 Ferrara, Italy
Phone: +39 0532 202.528
Fax: +39 0532 202.528
E-mail: lulombardo@tiscali.it